行政院國家科學委員會專題研究計畫　期中進度報告

複雜流體系統之研究:電腦模擬,理論及實驗之互補互成

(1/3)

計畫類別： 個別型計畫
計畫編號： NSC93-2113-M-009-015-
執行期間： 93 年 08 月 01 日至 94 年 07 月 31 日
執行單位： 國立交通大學應用化學系(所)

計畫主持人： 林銀潢

報告類型： 精簡報告

處理方式： 本計畫可公開查詢

中　華　民　國 94 年 5 月 27 日

國科會研究計畫進度報告 (May 25, 2005)
計畫名稱: 複雜流體系統之研究:電腦模擬,理論及實驗之互補互成(1/3)
(NSC93-2113-M-009-015-)
主持人: 林銀潢 教授, 國立交通大學應化系

The interplay of theory, experiment and simulation has been a main interest of my research project. Progresses in all three areas have been made to different degrees in the past one year. Linkages in certain aspects among the three have been made: (1) The theoretical analysis of the Plazek's creep compliance $J(t)$ results in both the entangled and entanglement-free regions; (2) The emergence of entropy-derived viscoelastic dynamics─Rouse normal modes of motion─from energetically interacting chains as revealed from the Monte Carlo simulation; (3) Comparison of the relaxation modulus $G(t)$ as extracted from Plazek's J_e^0 and $J(t)$ result in the entanglement-free region and that obtained from the Monte Carlo simulation. As these three research activities are taking up most of our human resources, a molecular dynamics simulation study on molecular motions in glass-forming binary fluids is temporarily coming to a halt while the computer programs for running the simulation under either NVE or NVT using the Nose–Hoover thermostat are developed; and some results at high temperatures are obtained whose validity is confirmed by comparison with literature. Before the molecular dynamics simulation work is resumed, a large disk storage capacity need be installed to our PC to facilitate the data handling. Below, I shall mainly highlight the three linkages between theory, experiment and simulation as mentioned above.

(1) Theoretical Analysis of the Creep Compliance *J*(*t*)

There are two main motives behind the analysis of Plazek's results: (1) Plazek's $J(t)$ results are very accurate and contain very rich information of polymer dynamics─from the glassy-relaxation region to the flow region. Even though his results are more than thirty years old, the rich information they contain has remained basically untapped. (2) Using the quantitatively successful description of the rubber(lik)-fluid region by the extended reptation theory (ERT) as the reference frame for analyzing the T_g-related dynamics that occurs in the short-time region of $J(t)$. This represents a totally new approach to studying the T_g-related dynamics.. The outcomes of the analysis are the understanding of the basic mechanism of the thermorheological complexity and the deduction that this basic mechanism should also be responsible for the break-down of the Stoke–Einstein relation occurring in glass-forming liquids as the glass-transition point is approached from above─a well-known effect that has been under intensive studies in the past decade. The analysis is quantitative; it explains the temporal unevenness of the thermorheological complexity naturally in a precise way. The study also shed light on the difference between the motion associated with a single Rouse segment and the T_g-related α Relaxation. In the past, due to the lack of clear definition of these two types of motion and the proximity of one to the other in the time scale, they could be easily confused. From this extensive study, two reports: "Whole Range of Chain Dynamics in Entangled Polystyrene Melts Revealed from Creep Compliance: Thermorheological Complexity between Glassy-Relaxation Region and Rubber-Fluid Region" and "Motion Associated with a Single Rouse Segment versus

the α Relaxation" were prepared. Probably because the two reports are long as a result of very comprehensive studies and contain several ground-breaking concepts and ideas, their reviews have been very slow coming. Anyway, their reviews were only recently received; the reports are revised in response to the review comments and sent back to Journal of Physical Chemistry. The abstracts of the two reports as well as their figures are attached in the following:

(A)
Whole Range of Chain Dynamics
in Entangled Polystyrene Melts Revealed from Creep Compliance:
Thermorheological Complexity
between Glassy-Relaxation Region and Rubber-Fluid Region

Y.-H. Lin
Department of Applied Chemistry
National Chiao Tung University
Hsinchu, Taiwan

Abstract
The rubber(like)-fluid region of the creep compliance $J(t)$ results reported by Plazek of two nearly monodisperse polystyrene melts in the entanglement region have been quantitatively analysed in terms of the extended reptation theory (ERT), giving the frictional factor K $(=\zeta\langle b^2\rangle/kT\pi^2m^2)$ in quantitative agreement with the values obtained previously from analysing the relaxation modulus $G(t)$ line shapes as well as calculated from the viscosity and diffusion data─a quantity shown independent of molecular weight as expected from the theory. Using the successful description of $J(t)$ in terms of ERT in the rubber(like)-fluid region as the *reference frame* in time, the glassy-relaxation process $\mu_G(t)$ that occurs in the small-compliance/short-time region of $J(t)$ can be studied in perspective. As shown from the analysis in terms of a stretched exponential form for $\mu_G(t)$ incorporated into ERT, the temperature dependence of the *energetic interactions-derived* $\mu_G(t)$ process being stronger in a simple manner than that of the *entropy-derived* ERT processes accounts fully for the uneven thermorheological complexity occurring in $J(t)$ as initially observed by Plazek. When the results of analysis being displayed in the $G(t)$ form, the relative roles of the energetic interactions-derived dynamic process and the entropy-derived ones in polystyrene are clearly revealed. It is shown that at the calorimetric glass transition temperature, T_g, the contribution from energetic interactions among segments to $G(t)$ at the time scale of the highest Rouse–Mooney normal mode greatly exceeds that derived from entropy, indicating vitrification at the Rouse-segmental level. At the same time the Rouse–Mooney normal modes provide an internal yardstick for estimating the characteristic length scale of a polymer at T_g, giving ~3 nm for polystyrene. Based on the obtained results, the basic mechanism for the thermorheological complexity occurring in polystyrene is analysed. It is shown that this basic mechanism should be also responsible for the breakdown of the Stoke -Einstein equation in relating the translational diffusion constant and viscosity as observed in glass-forming liquids, such as OTP and TNB, in approaching T_g from above.

Figure A1
Creep compliance $J(t)$ data of sample A measured at 114.5 (▵); 109.6 (•); 104.5 (◦); 100.6 (▾); and 97 (▿) ^{o}C in comparison with the theoretical curves (—— ; from left to right, respectively) calculated with K=5x10^{-9}, G_N=1.89x10^{6} dyne/cm^2; and the A_G, β and s values as explained and given in the text.

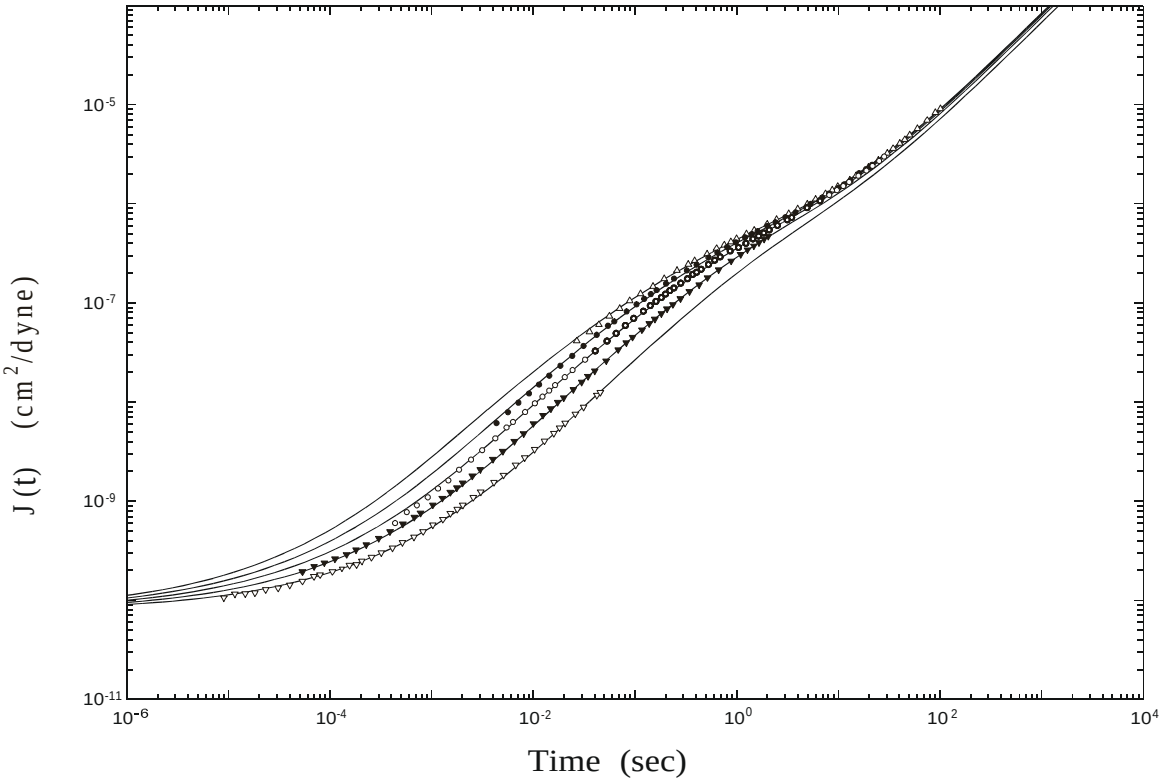

Figure A2
Creep compliance $J(t)$ data of sample B measured at 119.8 (▵); 113.8 (•); 105.5 (◦); 101.0 (▾); and 98.3 (▿) ^{o}C in comparison with the theoretical curves (—— ; from left to right, respectively) calculated with K=5x10^{-9}, G_N=1.89x10^{6} dyne/cm^{2} ; and the A_G, β and s values as explained and given in the text.

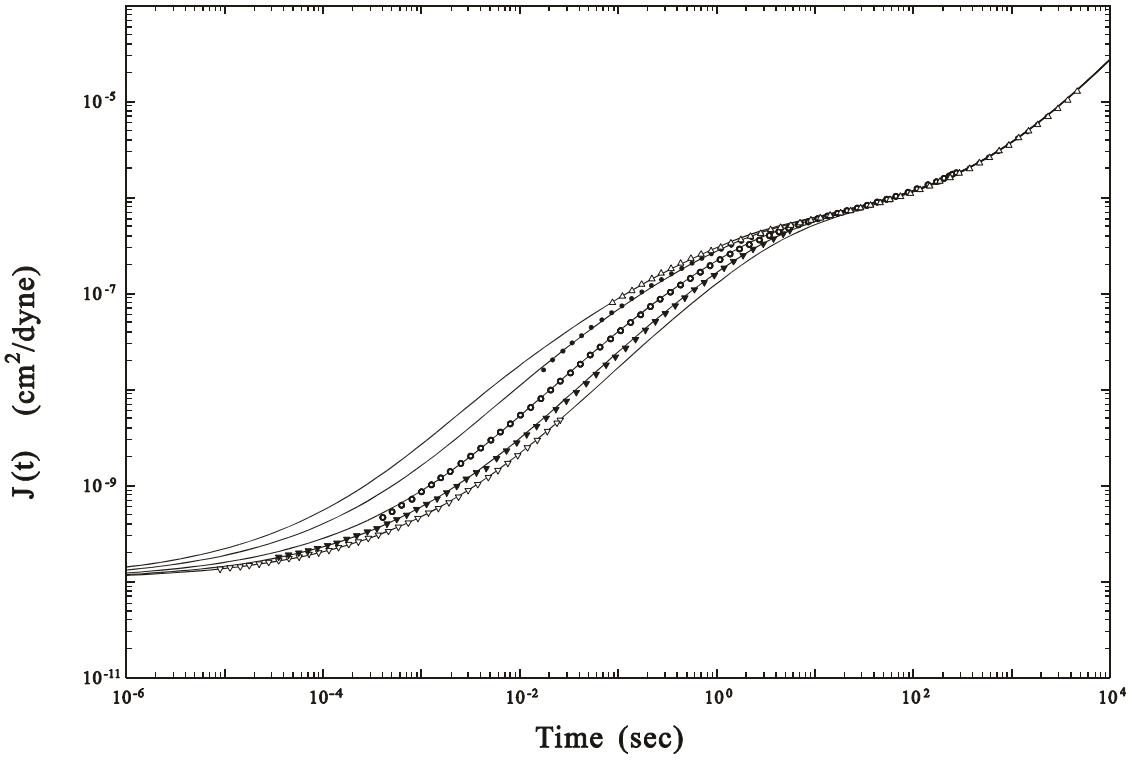

Figure A3
Comparison of the $J(t)$ curves calculated at β=0.36 (upper dashed line), 0.41 (solid line) and 0.46 (lower dashed line) with A_G=5482, s=56550; the one with β=0.41 is the same as the calculated curve shown in Figure 1 for sample A at 97^{o}C.

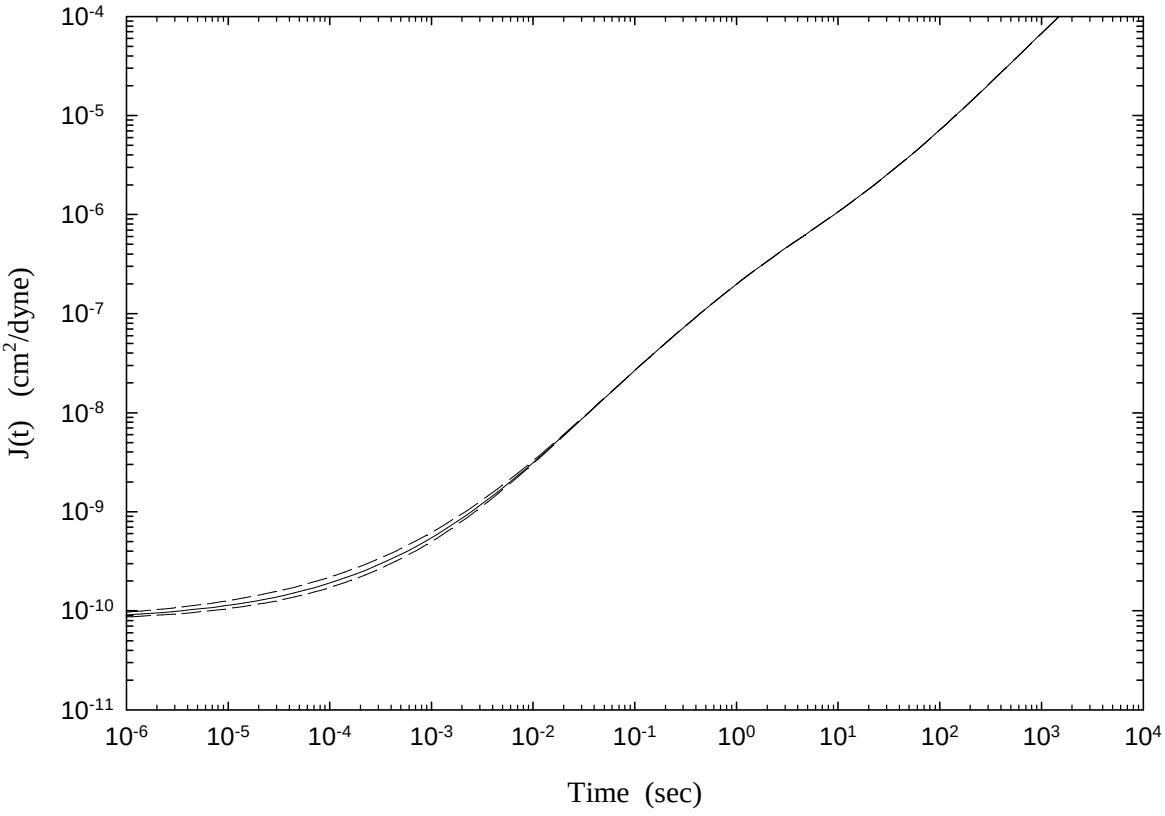

Figure A4
The normalized glassy-relaxation time *s* of samples A (◇) and B (○) at different temperatures. See the text.

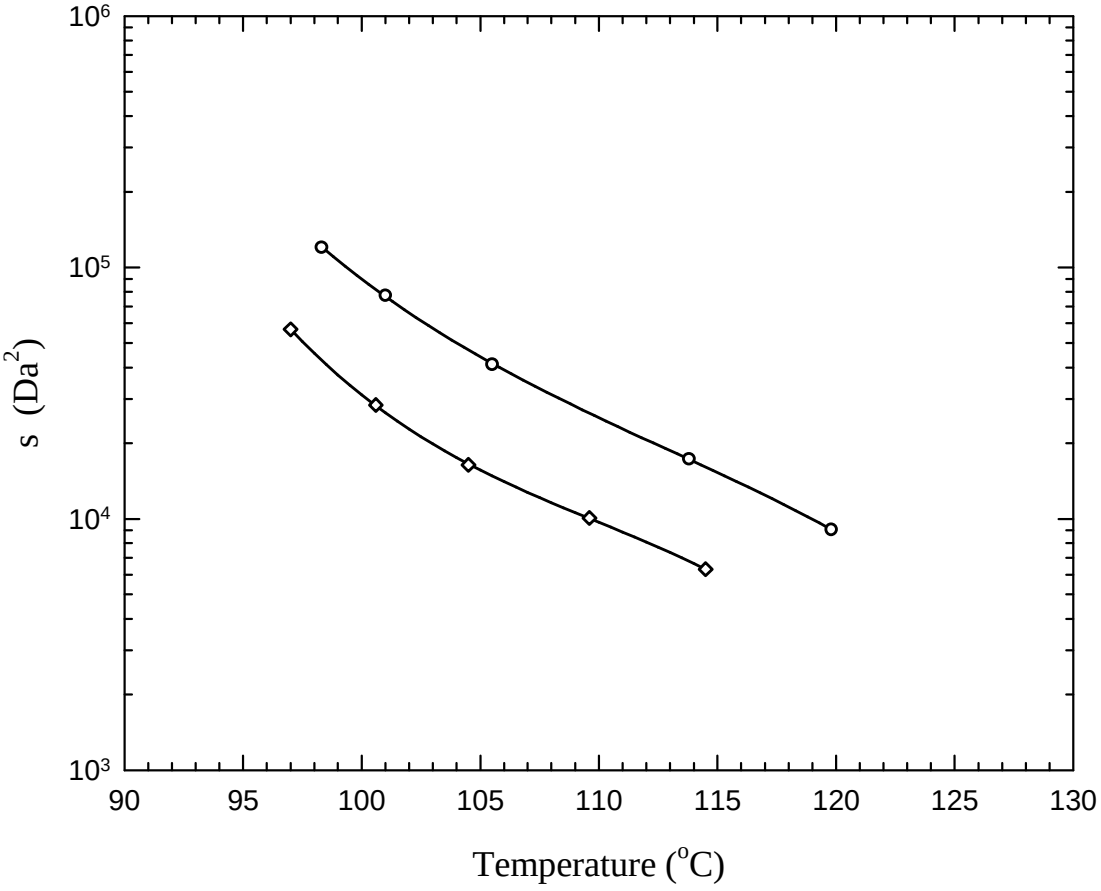

Figure A5
Comparison of the $G(t)$ (——) and $J(t)^{-1}$ (•••) curves for sample B at 113.8 ^{o}C (same $J(t)$ as the corresponding one shown in Figure 2). Also shown are the curves calculated without the $A_G\mu_G(t)$ process: (− − −) for $G(t)$ and (◦◦◦) for $J(t)^{-1}$; the dotted line indicates the $G(t)$ curve calculated without both the $A_G\mu_G(t)$ and $\mu_A(t)$ processes.

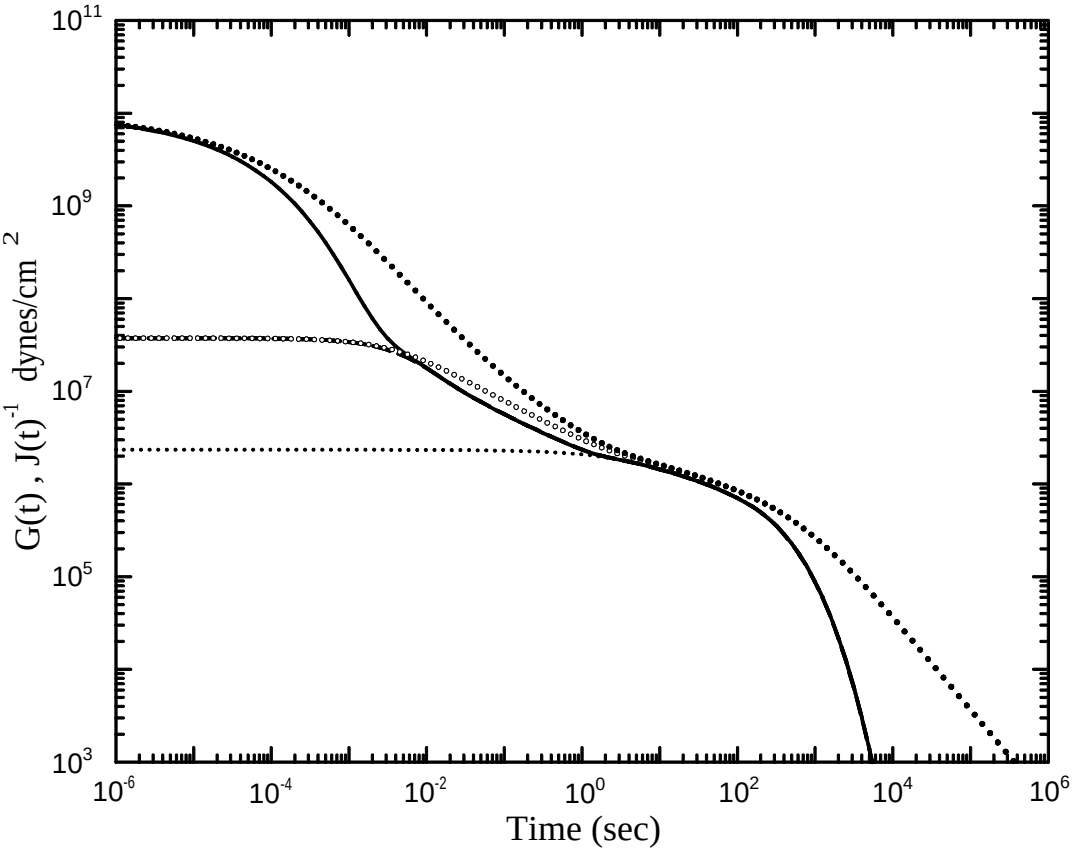

Figure A6
Calculated $G(t)$ curves corresponding to three $J(t)$ curves shown in Figure 1 for sample A: a for 114.5°C (——), b for 104.5°C (– · –), and c for 97°C (– · · –). Line d is calculated without the $A_G\mu_G(t)$ process; line e is calculated without both the $A_G\mu_G(t)$ and $\mu_A(t)$ processes. The (– – –) lines from bottom up represent the sums of line e and the first 3, 6, 9, and 12 modes in $\mu_A(t)$, respectively. The dots represent the locations of the relaxation times as indicated. In the three dots under $\langle\tau\rangle_G$, the left one is for a; the middle one, for b; and the right one, for c.

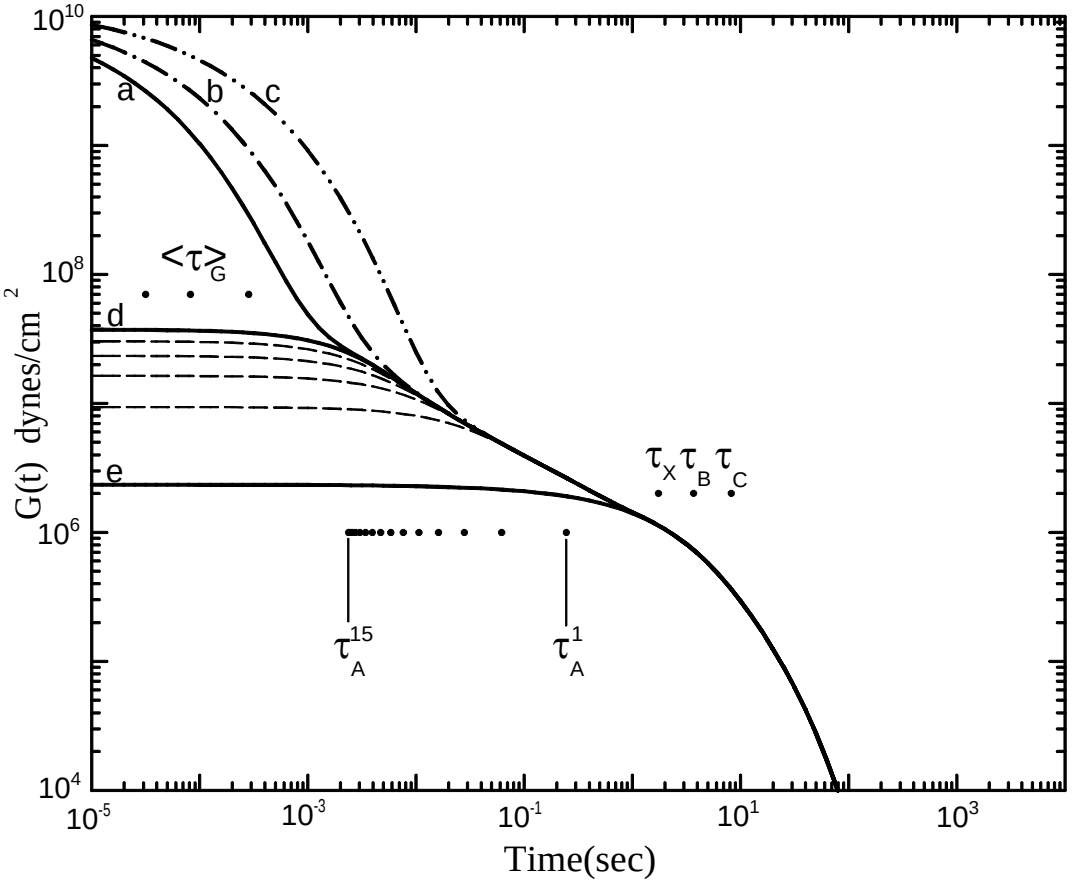

Figure A7
Calculated $G(t)$ curves corresponding to three $J(t)$ curves shown in Figure 2 for sample B: a for 113.8°C (——), b for 105.5°C (– · –), and c for 98.3°C (– · · –). The rest are the same as in Figure 6.

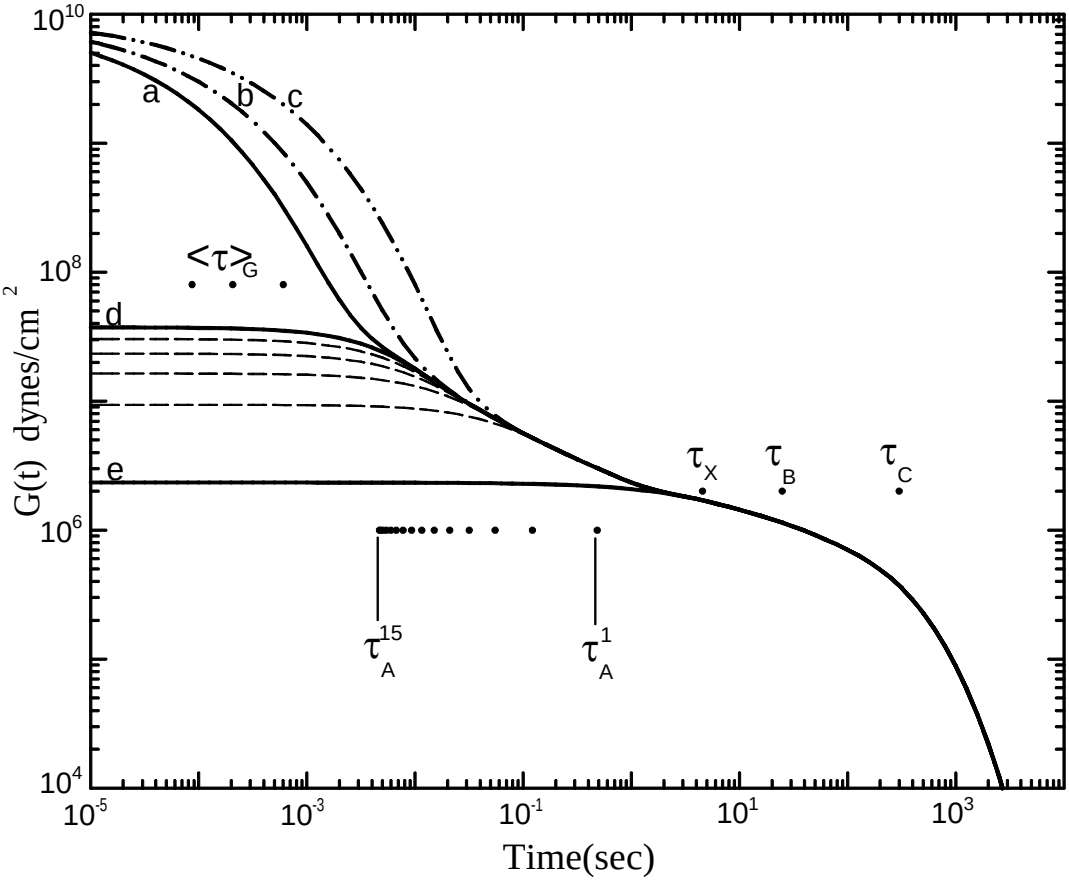

(B)
Motion Associated with a Single Rouse Segment versus the α Relaxation

Y.-H. Lin
Department of Applied Chemistry
National Chiao Tung University
Hsinchu, Taiwan

Abstract

The dynamics in polystyrene melt and concentrated solution as probed by depolarized photon-correlation spectroscopy has been shown to reflect the motion associated with a single Rouse segment. In the concentrated-solution case (entanglement-free), the analysis using the frictional factor K ($=\zeta\langle b^2\rangle/kT\pi^2m^2$) extracted from the viscosity data in terms of the Rouse theory and aided by the Monte Carlo simulation based on the Langevin equation of the Rouse model confirms the conclusion in a precise manner. In the melt case (entangled), the Rouse-segmental motion as observed by depolarized photon-correlation spectroscopy is compared with the α relaxation and the highest Rouse–Mooney normal mode extracted from analyzing the creep compliance $J(t)$ of sample A reported in the previous paper. Another well-justified way of defining the structural- (α-) relaxation time is shown basically physically equivalent to the one used previously. Based on the analysis, an optimum choice $\tau_S = 18\langle\tau\rangle_G$ ($\langle\tau\rangle_G$ being the average glassy-relaxation time) is made, reflecting both the temperature dependence of $\langle\tau\rangle_G$ and the effect on the bulk mechanical property by the glassy-relaxation process. In terms of thus defined τ_S, two traditional ways of defining the α-relaxation time are compared and evaluated. It is shown that as the temperature approaches the calorimetric T_g, two *modes of temperature dependence* are followed by the dynamic quantities concerning this study: One includes the time constant of the highest Rouse–Mooney normal mode, τ_v; the temperature dependence of the viscosity corrected for the changes in density and temperature, $\eta/\rho T$; and the average correlation time obtained by depolarized photon-correlation spectroscopy, $\langle\tau_c\rangle$. The other, being steeper, is followed by the α-relaxation time τ_S derived from the glassy-relaxation process, and the temperature dependence of the recoverable compliance $J_r(t)$ as obtained by Plazek. The comparison of the dynamic quantities clearly differentiates the motion associated with a single Rouse segment as characterized by τ_v or $\langle\tau_c\rangle$ from the α relaxation as characterized by τ_S; due to the lack of clear definition of these two types of motion in the past and the proximity of one to the other in the time scale—actually the two crossing over each other—as the temperature is approaching T_g, the two modes could be easily confused. Below ~110°C, the rate of $\langle\tau_c\rangle$ changing with temperature lags behind that of τ_v is explained as due to the loss of effective ergodicity taking place in the system.

Figure B1
Comparison of the $\langle P_2\ [\mathbf{u}(0)\cdot\mathbf{u}(t)]\rangle^2$ dynamic processes obtained from the depolarized photon-correlation functions of the S1 (◦)and S2 (•) samples and the simulation results of the Rouse chain with N_r=8 (the left solid line) and with N_r=16 (the right solid line).

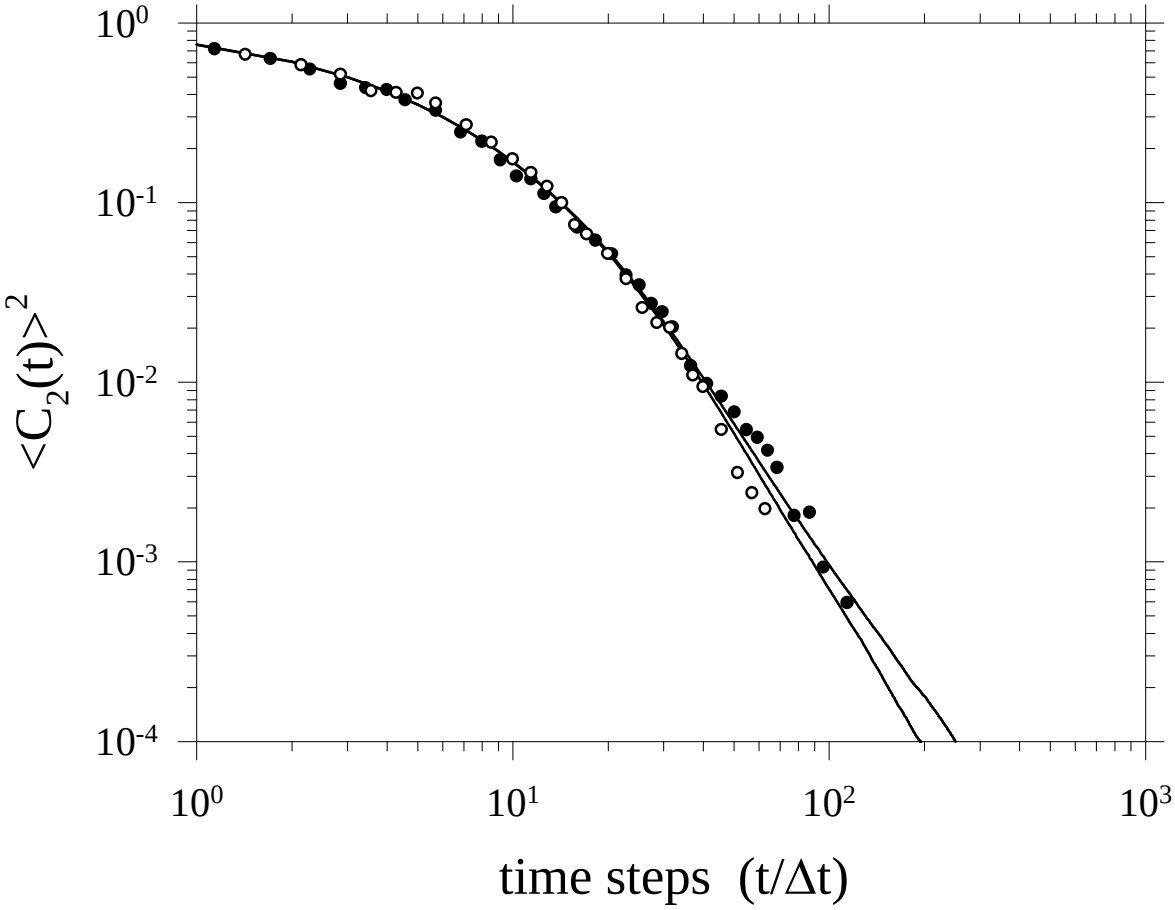

Figure B2
H indicating the declining rate of log *G*(*t*) vs. log *t*, as defined in the text, is shown as a function of time for sample A at 114.5, 109.6, 104.5, 100.6, and 97^{o}C corresponding to lines from left to right, respectively; all calculated with *K* fixed at 5x10^{-9} and the respective *s* values listed in Table 1.

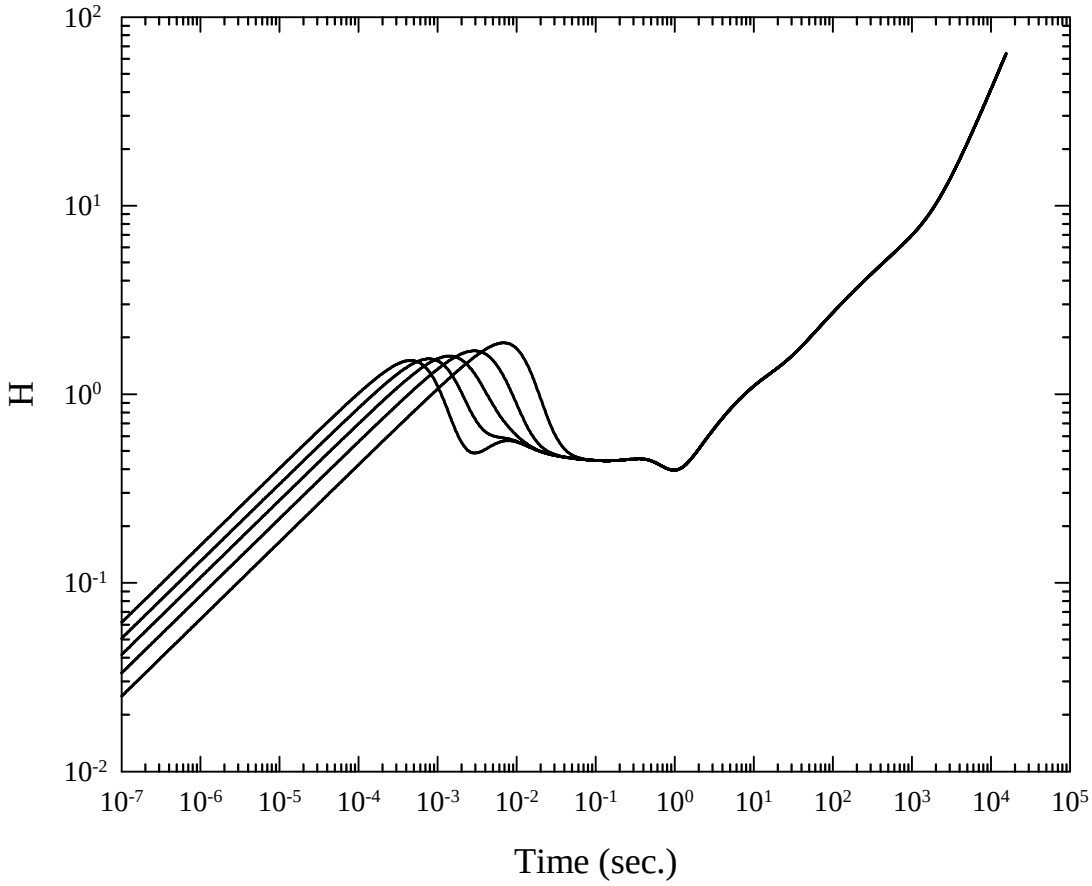

Figure B3
Comparison of the storage- and loss-modulus spectra, $G'(\omega)$ and $G''(\omega)$, of sample A at 114.5 (——), 104.5 (– · –), and 97°C (–··–) all calculated with K fixed at 5×10^{-9} and the respective s values listed in Table 1.

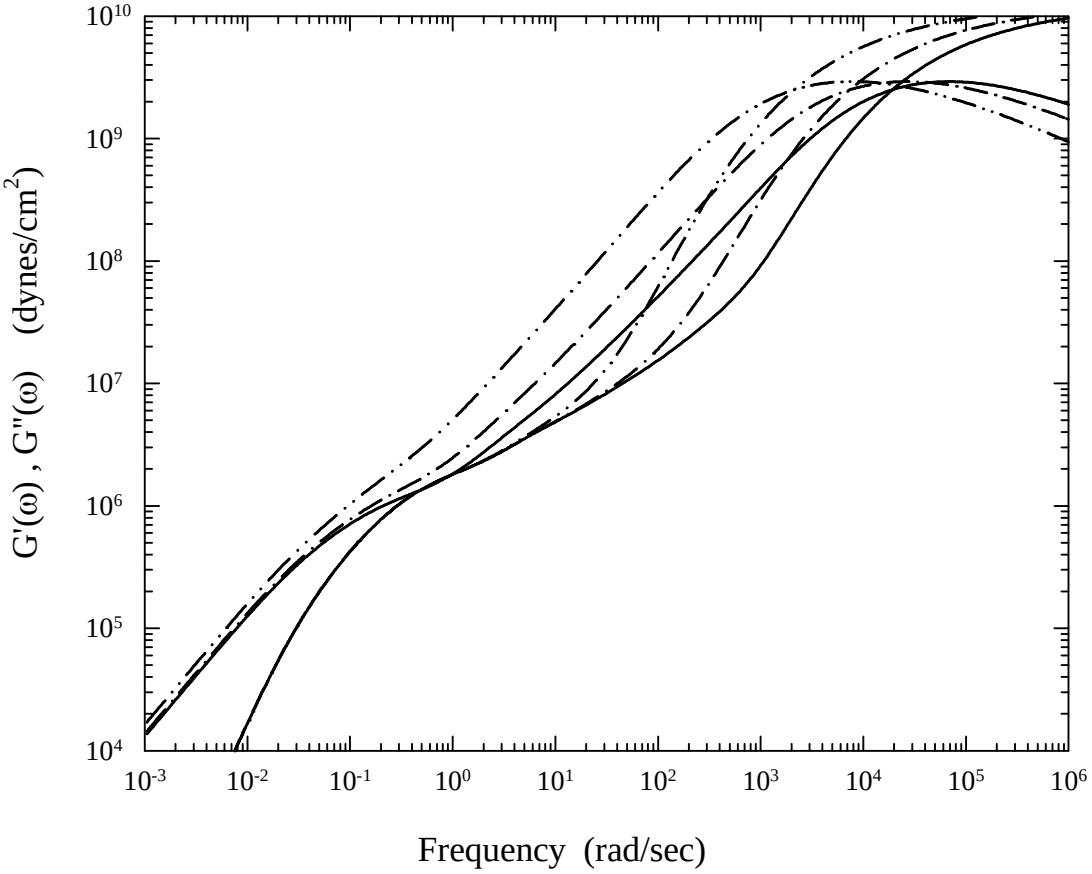

Figure B4
Comparison of the storage-modulus (——) and loss-tangent (– – –) spectra of sample corresponding to those shown in Fig. 3: a for 114.5°C, b for 104.5°C and c for 97 °C. Also shown are the $\omega_S=0.7/\tau_S$ values (right ↓ for a; middle ↓ for b; left ↓ for c) calculated with K fixed at $5\text{x}10^{-9}$ and the respective s values listed in Table 1; and the $\omega_v=0.7/\tau_v$ value (↑) calculated with the same K. The upper dotted line is $G'(\omega)$ calculated without the $A_G\mu_G(t)$ term; the lower dotted line is calculated without both $A_G\mu_G(t)$ and $\mu_A(t)$.

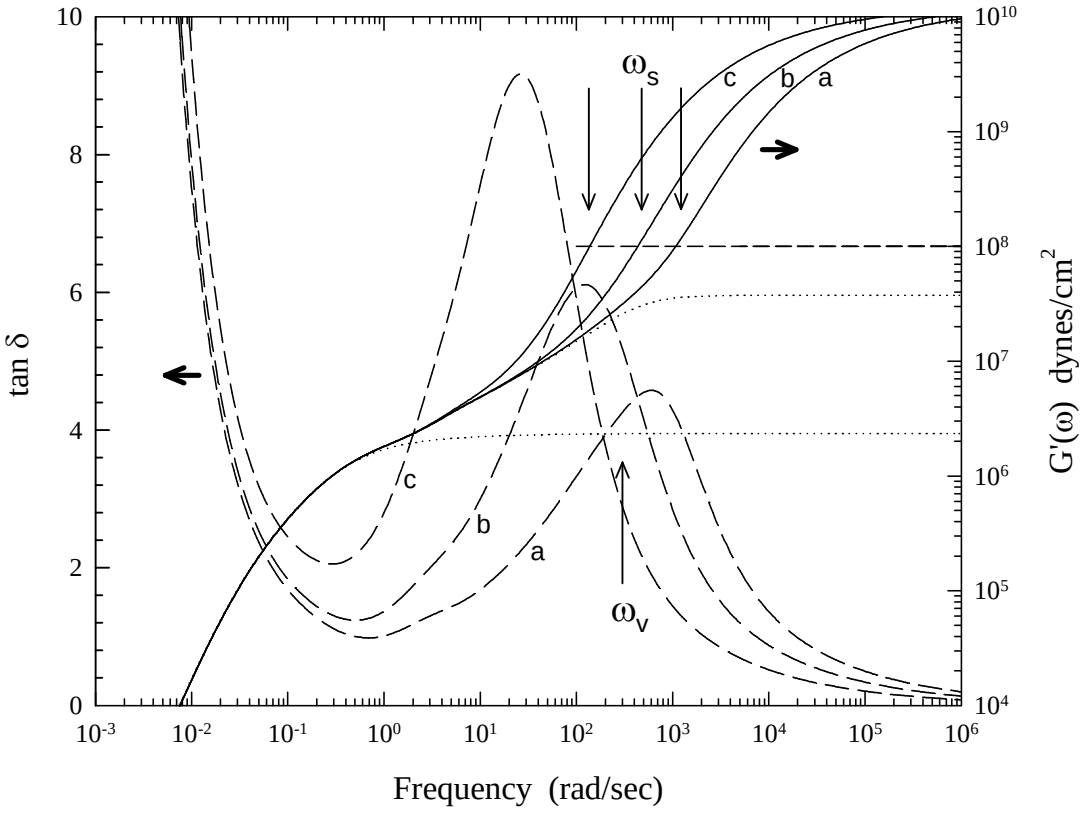

Figure B5
Comparison of τ_v (●), $0.77\langle\tau_c\rangle$ (■) and τ_S (○) as a function of temperature with the temperature dependence of $\eta/\rho T$ (——; the extended line below 104.5°C is indicated by · · ·) and $J_r(t)$ (— · — · —); see the text.

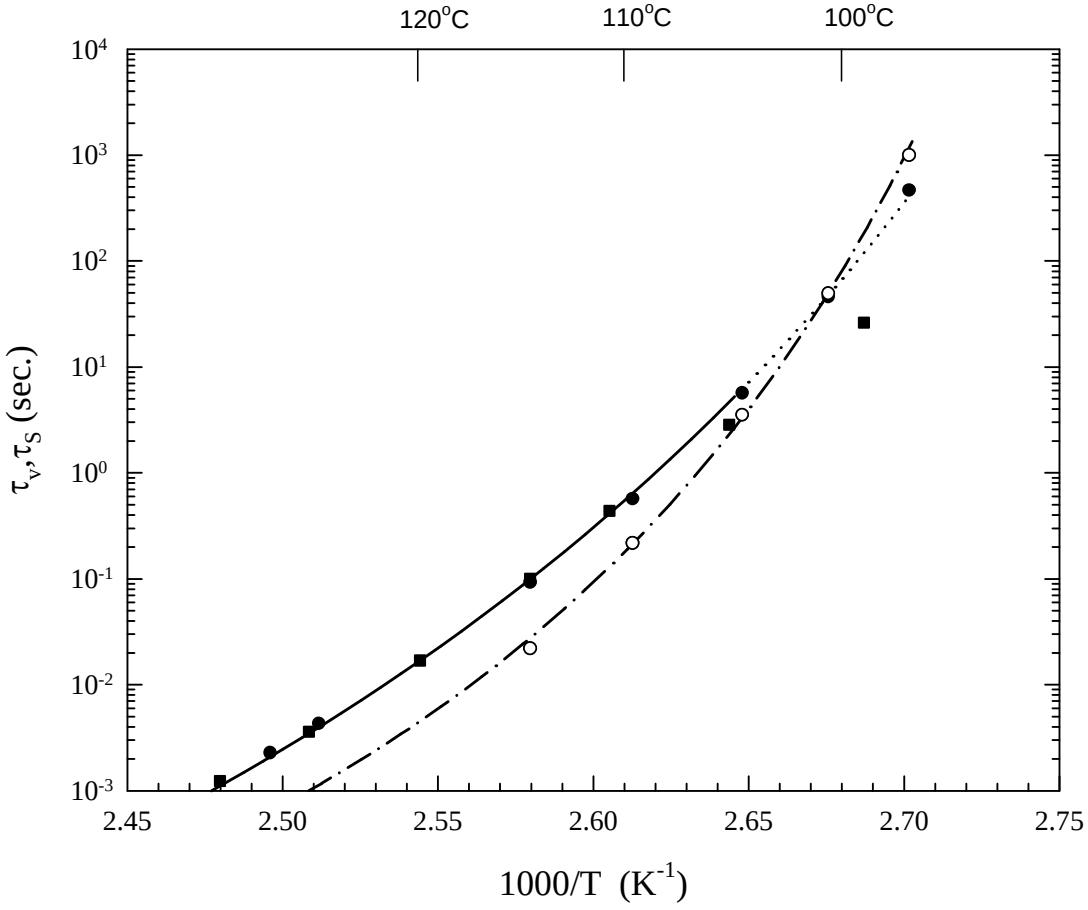

(C)

Analysis of J_e^0 and $J(t)$ of an Entanglement-Free Polystyrene Melt

As used to analyze the $J(t)$ results in the entangled region and reported in the Thermorheological Complexity paper mentioned above, a similar analysis scheme is developed to analyze the steady-state compliance J_e^0 data and the $J(t)$ result of Plazek in the entanglement-free region. The basic difference is the replacement of ERT by the Rouse theory. In both the entangled and entanglement-free region, the thermorheological complexity is characterized by the single parameter *s*, defined as the ratio of the average glassy-relaxation time to the frictional factor *K*. *s* increases with decreasing temperature, reflecting the stronger temperature dependence of the energetic interactions-derived dynamic process, the glassy relaxation, in comparison to the entropy-derived dynamics. As shown in Figure C1, *s* rises in a similar way as the temperature approaches T_g from above for three different molecular weights: 3400($T_g \approx 70^oC$), 46900($T_g \approx 97^oC$) and 122000($T_g \approx 98^oC$)–one molecular weight (3400) in the entanglement-free region and two (46900 and 122000) in the entangled region, indicating the universality of the way in which the thermorheological complexity exists in polystyrene. A report on this subject is under preparation.

Figure C1. Increase in s as the temperature approaching T_g from above, for three different molecular weights: 3400 (Δ); 46900(□); and 122000 (○).

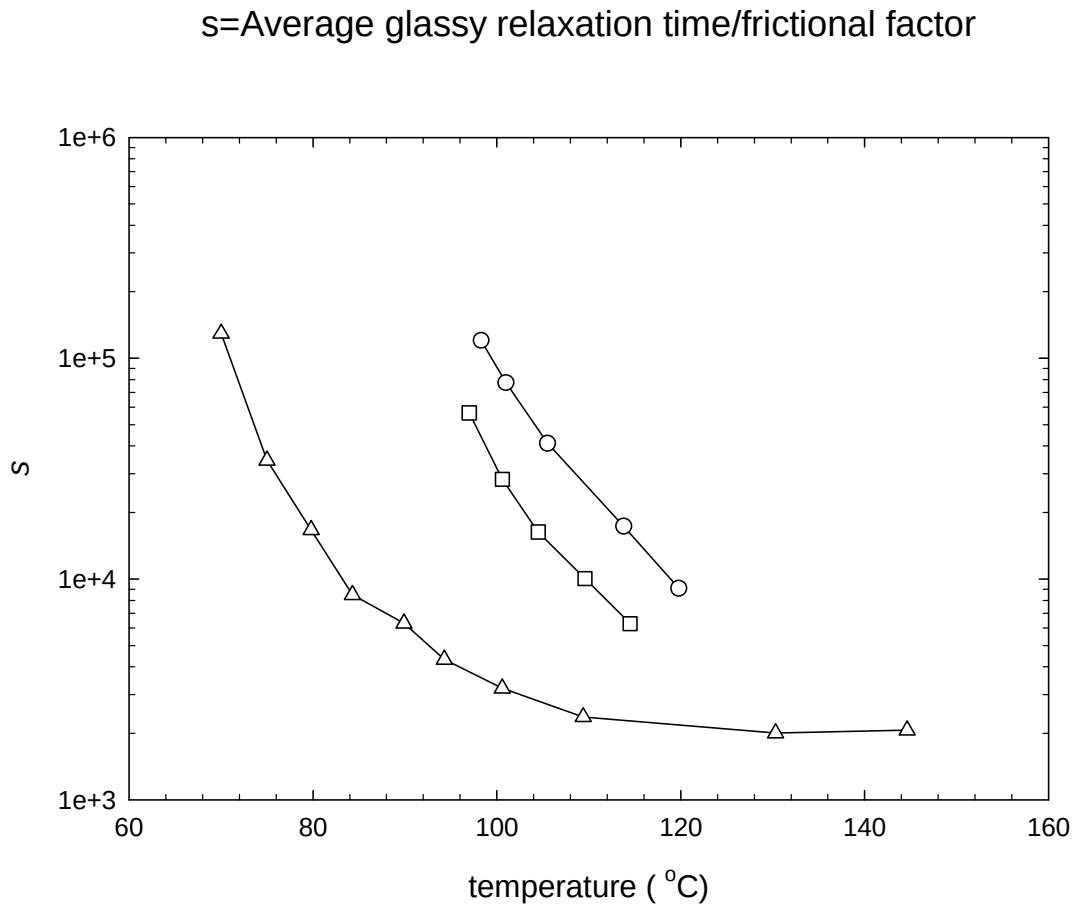

(2) Computer Simulation

(D)

Emergence of Entropy-Derived Viscoelastic Dynamics–Rouse Normal Modes of Motion–from Energetically Interacting Chains as Revealed from the Monte Carlo Simulation.

In the Rouse model, only the interaction between nearest neighboring beads described by

$$V(\{\mathbf{R}_n\}) = \frac{3kT}{2b^2}\sum_{n=1}^{N}(\mathbf{R}_{n+1}-\mathbf{R}_n)^2 \qquad \text{(D1)}$$

is considered. Based on the functional form of the potential, the distance between two connected beads would collapse to zero if there were no thermal fluctuations. Here, the interactions of each bead with its surrounding will be modeled in a way more analogous to a real concentrated polymer solution system. The results of simulations on such systems may shed light on why the theories using the Rouse segment as the most basic structural unit–the Rouse theory and the extended reptation theory–are so successful in describing the viscoelastic responses of concentrated polymer solution systems in the frequency region below that corresponding to the motion associated with a single Rouse segment, which will be referred to as the entropic region below.

We consider a system consisting of c chains, each with N beads, in a cubic box of length L on each side. In order to mimic the presence of an infinite bulk surrounding the c chains, the periodic boundary condition is applied; namely, at the coordinates:

$$x \pm nL, \quad y \pm nL, \quad z \pm nL; \qquad \text{with } n \text{ being any integer,}$$

there exist beads identical to those at (x, y, z). Each bead interacts with its nearest neighbors in the same chain through the Fraenkel potential:

$$V_{\mathrm{F}}\left(\mathbf{R}_{n+1}^{k}-\mathbf{R}_{n}^{k}\right) = \frac{H_F}{2}\left(\frac{\left|\mathbf{R}_{n+1}^{k}-\mathbf{R}_{n}^{k}\right|}{b_0}-1\right)^2 \qquad \text{(D2)}$$

(the chain is labeled by the superscript index: k or l; the bead by the subscript index: n or m) where H_{F} is the force constant and b_0 is the bond length at which the potential is at its minimum or the tension on the bond is zero; and interacts with all other beads, belonging to the same chain or not, through the truncated and shifted Lennard–Jones (LJ) potential:

$$\begin{aligned} V_{\mathrm{ST}}(\mathbf{r}_{nm}^{kl}) &= V_{\mathrm{LJ}}(\mathbf{r}_{nm}^{kl}) - V_{\mathrm{LJ}}(r_{\mathrm{c}}) \qquad \text{for } \left|\mathbf{r}_{nm}^{kl}\right| \le r_{\mathrm{c}} \\ &= 0 \qquad\qquad\qquad\qquad\quad \text{for } \left|\mathbf{r}_{nm}^{kl}\right| > r_{\mathrm{c}} \end{aligned} \qquad \text{(D3)}$$

with r_{c} set at 2.5σ and

$$V_{\mathrm{LJ}}(\mathbf{r}_{nm}^{kl}) = 4\varepsilon\left[\left(\sigma/\left|\mathbf{r}_{nm}^{kl}\right|\right)^{12} - \left(\sigma/\left|\mathbf{r}_{nm}^{kl}\right|\right)^{6}\right] \qquad \text{(D4)}$$

where ϵ is the depth of the potential well; $\mathbf{r}^{kl}_{nm} = \mathbf{R}^{l}_{m} - \mathbf{R}^{k}_{n}$ for all n and m when $k \neq l$ and $|n-m| \geq 2$ when $k=l$; and σ is the inter-bead distance at which the potential is zero. σ may be used to define the concentration or volume fraction, ϕ, of the studied system:

$$\phi = \frac{cN\pi\sigma^3}{6L^3} \qquad \text{(D5)}$$

In the simulation, the beads of all the chains in the cube are labeled and their movements are followed. At each time-step, the center of mass of each of these chains is checked and will be converted to its image inside the cubic box by applying the periodic boundary condition, if it is not already in the box. For easily calculating the Fraenkel potential force between two neighboring beads, no chain is separated into two parts–i.e. on the opposite surfaces of the box separated by the distance L. As a result, some of the labeled beads may be outside of the cubic box; however, they cannot go beyond a distance, $\sim(N/2)^{.5}b_0$, from the surface of the box. This does not cause a problem in calculating the forces on these labeled beads as required in following their movements, as the minimum distance between any two beads can be automatically used in calculating the LJ interaction forces in the simulation program–by subtracting L automatically from the absolute value of any component of $\mathbf{r}^{kl}_{nm}$ whenever it has a value greater than L. The simulation is run using parallel processing with each cpu responsible for the time-evolution of an individual chain.

The non-random force on each bead in the Langevin equation represents the sum of forces derived from all kinds of interactions. Then the Langevin equation for a bead can be written as

$$\frac{d\mathbf{R}^{k}_{n}}{dt} = \frac{\mathbf{F}^{k}_{n}}{\zeta} + \mathbf{g}^{k}_{n}(t) \qquad \text{(D6)}$$

where $\mathbf{F}^{k}_{n}$ is the sum of potential forces exerted on the bead, $\mathbf{R}^{k}_{n}$; and the fluctuation $\mathbf{g}^{k}_{n}(t)$ is defined by:

$$\langle \mathbf{g}^{k}_{n}(t) \rangle = 0 \qquad \text{(D7)}$$

and

$$\langle \mathbf{g}^{k}_{n}(t')\mathbf{g}^{l}_{m}(t'') \rangle = \frac{2kT}{\zeta}\mathbf{I}\delta_{kl}\delta_{nm}\delta(t'-t'') \qquad \text{(D8)}$$

$\mathbf{F}^{k}_{n}$ can be expressed as the sum of three types of forces:

$$\mathbf{F}_n^k = \mathbf{F}_{\mathrm{F},n}^k + \mathbf{F}_{\mathrm{LJ},n}^k + \mathbf{F}_{\mathrm{LJ},n}^{\neq k} \qquad \text{(D9)}$$

where $\mathbf{F}_{\mathrm{F},n}^k$ is the Fraenkel force; $\mathbf{F}_{\mathrm{LJ},n}^k$ the LJ force between beads belonging to the same chain; and $\mathbf{F}_{\mathrm{LJ,n}}^{\neq k}$ the LJ force between beads not belonging to the same chain.

With H_{F} and ϵ expressed in unit of kT, Eq. (D6) can be transformed into

$$\mathbf{R}_n^k(i+1) = \mathbf{R}_n^k(i) + \frac{d^2}{2}\mathbf{F}_n^k(i) + \mathbf{d}_n^k(i) \qquad \text{(D10)}$$

with

$$\langle \mathbf{d}_n^k(i) \rangle = 0 \qquad \text{(D11)}$$

$$\langle \mathbf{d}_n^k(i)\mathbf{d}_m^l(j) \rangle = d^2\mathbf{I}\delta_{kl}\delta_{nm}\delta_{ij} \qquad \text{(D12)}$$

For studying the stress relaxation behavior of the c chains, each with N beads, confined inside a L^3 cubic box as described above, a step shear deformation as given by

$$\mathbf{E} = \begin{pmatrix} 1 & \lambda & 0 \\ 0 & 1 & 0 \\ 0 & 0 & 1 \end{pmatrix} \qquad \text{(D13)}$$

is applied to the configuration of the chains denoted by $\{\mathbf{R}^k{}_n(0-)\}$in an equilibrium state at t_i=0, using the affine-deformation assumption. In carrying out the execution of Eq. (D10) following a step deformation, the coordinates of and forces on all the individual beads, $\{\mathbf{R}^k{}_n(i)\}$ and $\{\mathbf{F}^k{}_n(i)\}$, at each time-step i are calculated. Then the stress tensor $\boldsymbol{\tau}(i)$ at the ith time-step following the step deformation at t_i=0 is calculated by

$$\boldsymbol{\tau}(i) = \frac{1}{V}\sum_{k=1}^{c}\sum_{n=1}^{N}\overline{\mathbf{F}_n^k(i)\mathbf{R}_n^k(i)} \qquad \text{(D14)}$$

where the bar denotes averaging the quantity under it over the repetition of applying a step shear strain at t_i=0. The initial deformed configuration $\{\mathbf{R}^k{}_n(0+)\}$ is created numerically from$\{\mathbf{R}^k{}_n(0-)\}$ by the application of the affine deformation. Such a numerical process may be different from a physical situation, where potential barriers may be encountered during the deformation. Here, the numerically created affine deformation is a part of our model system; it should not affect in a substantial way the main point which the simulation is intended to illustrate.

Shown in Figures D1 and D2 are stress relaxation modulus results obtained from the simulation for the systems consisting of 9-beads chains and consisting of 5-beads chains, respectively. The relaxation curves clearly display two major relaxation processes. The

slow one is closely described by the Rouse relaxation (solid lines) expected for chains with 9 beads and 5 beads, respectively. Not only the dependence of relaxation time on the number of beads follows that given by the Rouse theory, the modulus is of the order of magnitude expected from the entropy force constant on the Rouse segment. More simulations need be carried out before we can better understand the basic physics behind the emergence of the entropy-derived dynamics from energetically interacting chains. Such studies may shed light on why the theories using the Rouse segment as the most basic structural unit–the Rouse theory and the extended reptation theory–are so successful in describing the viscoelastic responses of concentrated polymer solution systems in the long-time region.

Figure D1. Comparison of the stress relaxation modulus obtained from the Monte Carlo simulation (◦) and that calculated from the Rouse theory (—) in the long-time region for a system consisting of chains with 9 beads.

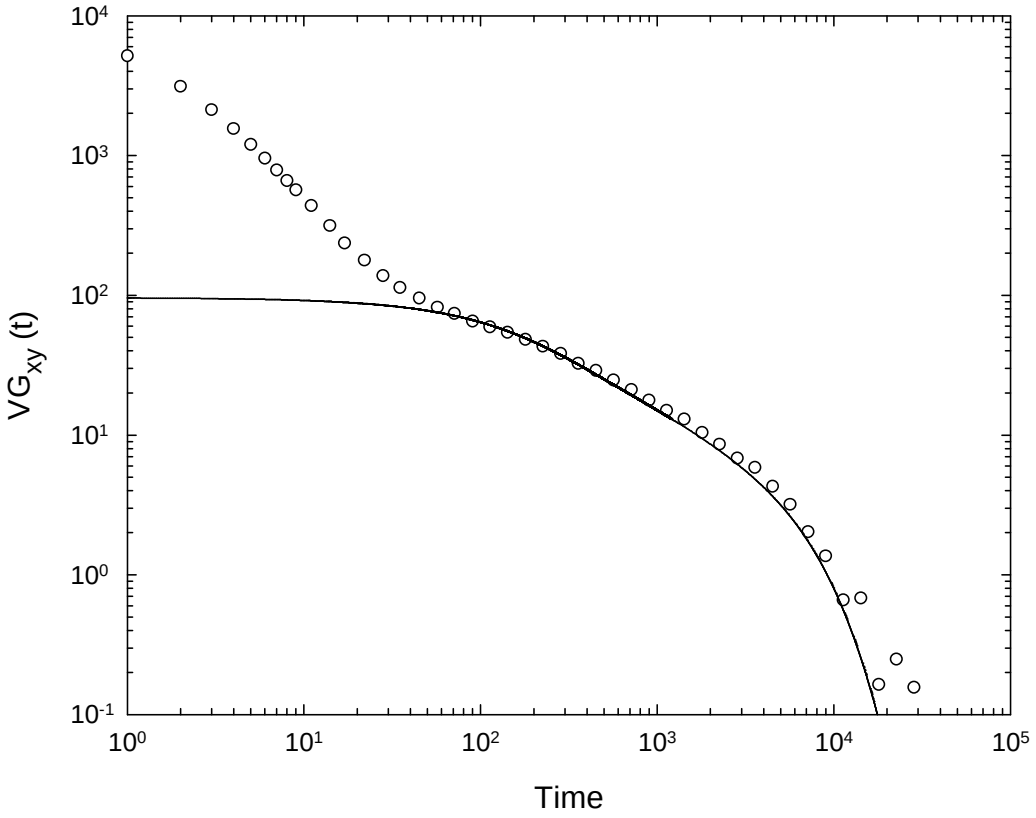

Figure D2. Comparison of the stress relaxation modulus obtained from the Monte Carlo simulation (◦) and that calculated from the Rouse theory (—) in the long-time region for a system consisting of chains with 5 beads.

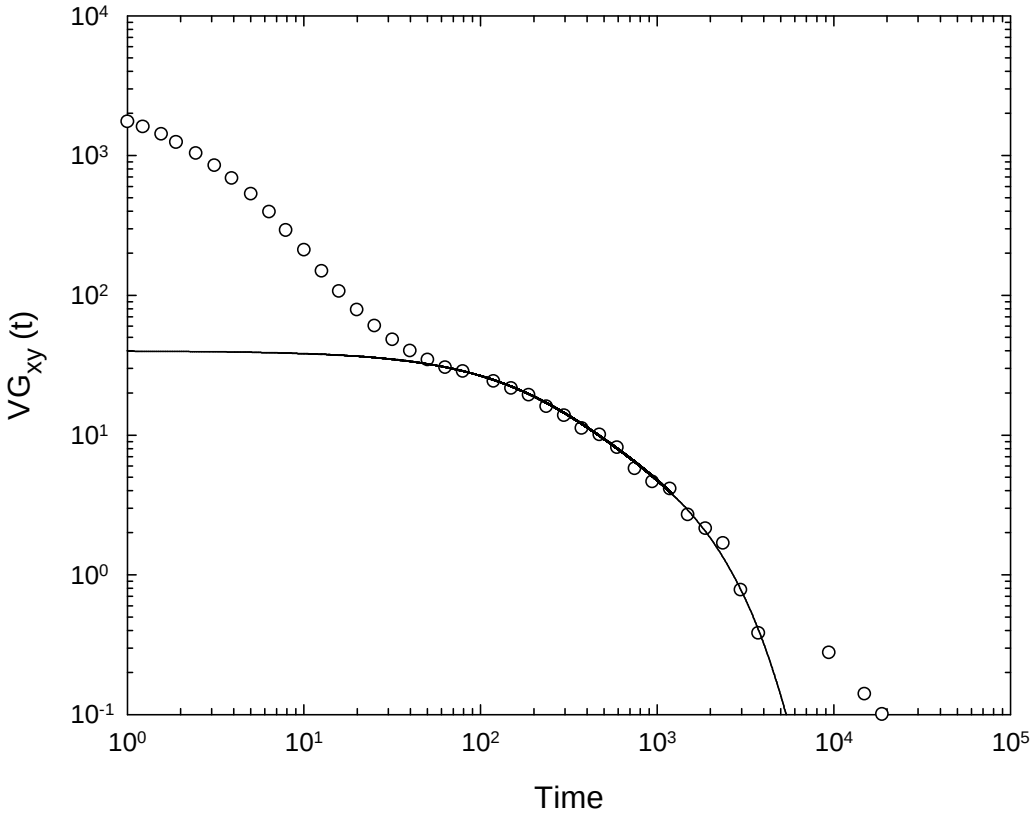

Comparison of Simulation and Experiment

(E)

Comparison of $G(t)$ from Simulation and That Extracted from $J(t)$ and J_e^0

The relaxation modulus $G(t)$ is related to $J(t)$ and J_e^0 through the following equations:

$$t = \int_0^t J(t')G(t-t')dt'$$

$$J_e^0 = \frac{\int_0^\infty G(t)tdt}{\left[\int_0^\infty G(t)dt\right]^2}$$

Using the above two equations, $G(t)$ has been extracted from the $J(t)$ and J_e^0 results of Plazek for a nearly monodisperse polystyrene sample with MW=3400. The mass of a Rouse segment is about 850; thus, the studied sample is equivalent to a system consisting of Rouse chains with 5 beads. Shown in Figure E1 is the comparison of the $G(t)$ extracted from the $J(t)$ and J_e^0 data and that obtained from the Monte Carlo simulation as described in (D) for the 5-beads chain. The overall agreement between the simulation and the experimental result is very encouraging; the agreement between the two may suggest a generic pattern for the viscoelastic behavior of a flexible linear polymer and the fundamental ingredients for its rising.

Figure E1. Comparison of $G(t)$ extracted from the $J(t)$ and J_e^0 results (—) of a nearly monodisperse polystyrene sample with MW=3400 and that obtained from the Monte Carlo simulation for a system consisting of chains with 5 beads (◦). In the superposition process, a shift has been applied to the simulation result along both the modulus and time axes.